

# Successful Virtual Screening for a Submicromolar Antagonist of the Neurokinin-1 Receptor Based on a Ligand-Supported Homology Model

Andreas Evers<sup>†</sup> and Gerhard Klebe\*

Institut für Pharmazeutische Chemie, Philipps-Universität Marburg, Marbacher Weg 6, 35032 Marburg, Germany

Received December 18, 2003

The neurokinin-1 (NK1) receptor belongs to the family of G-protein-coupled receptors (GPCRs), which represents one of the most relevant target families in small-molecule drug design. In this paper, we describe a homology modeling of the NK1 receptor based on the high-resolution X-ray structure of rhodopsin and the successful virtual screening based on this protein model. The NK1 receptor model has been generated using our new MOBILE (modeling binding sites including ligand information explicitly) approach. Starting with preliminary homology models, it generates improved models of the protein binding pocket together with bound ligands. Ligand information is used as an integral part in the homology modeling process. For the construction of the NK1 receptor, antagonist CP-96345 was used to restrain the modeling. The quality of the obtained model was validated by probing its ability to accommodate additional known NK1 antagonists from structurally diverse classes. On the basis of the generated model and on the analysis of known NK1 antagonists, a pharmacophore model was deduced, which subsequently guided the 2D and 3D database search with UNITY. As a following step, the remaining hits were docked into the modeled binding pocket of the NK1 receptor. Finally, seven compounds were selected for biochemical testing, from which one showed affinity in the submicromolar range. Our results suggest that ligand-supported homology models of GPCRs may be used as effective platforms for structure-based drug design.

## Introduction

The NK1 receptor belongs to the family of tachykinin-binding receptors (NK1, NK2, and NK3). They selectively bind the peptide neurotransmitters substance P, neurokinin A, and neurokinin B, respectively. Substance P plays a role in the transmission of pain and is involved in inflammation and immune response. The NK1 receptor is a member of the superfamily of G-protein-coupled receptors (GPCRs) which mediate responses to, e.g., visual, olfactory, hormonal, or neurotransmitter signals. GPCRs represent one of the most relevant target families in small-molecule drug design. Currently, 50% of all marketed drugs address GPCRs.<sup>1</sup> Due to the fact that GPCRs are membrane-bound proteins, their expression, purification, crystallization, and structure determination remain a major enterprise. So far, only the structure of bovine rhodopsin could be determined to sufficiently high resolution.<sup>2</sup> Its crystal structure serves as a template reference for homology modeling of all other members of the GPCR family. The obtained models exhibit only limited accuracy; accordingly, successful computer-aided drug discovery for GPCRs was mainly achieved by applying ligand-based virtual screening techniques.<sup>3,4</sup> However, it was demonstrated that ligand binding at GPCRs can be rationalized with the aid of homology models based on rhodopsin. In several studies, the modeled receptor pocket conformations were validated or improved via docking of one or several

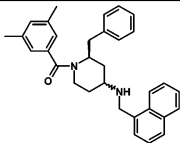
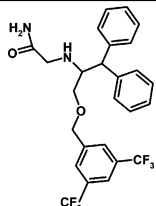
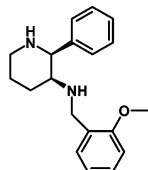
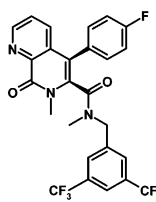
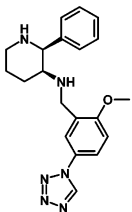
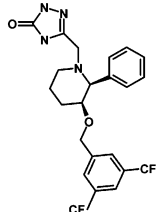
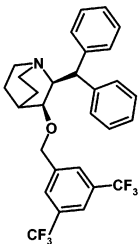
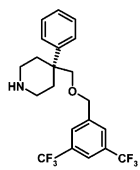
known ligands.<sup>5,6</sup> Drug discovery based on virtual screening with rhodopsin-based GPCR models has been reported only rarely in the literature.<sup>7–9</sup> Bissantz et al.<sup>7</sup> recently demonstrated that their homology models of the dopamine D3, muscarinic M1, and vasopressin V1a receptors were reliable enough to retrieve known antagonists via virtual screening from a database, which also comprised randomly selected drug-like molecules. Becker et al. applied a GPCR modeling technique, PREDICT, that does not rely on the crystal structure of bovine rhodopsin.<sup>8</sup> When screening for novel binders based on their GPCR models, the authors report hit rates of 10–24% success. Very recently, Varady et al. reported on an impressive discovery of novel potent D3 ligands using a hybrid pharmacophore- and structure-based database searching approach.<sup>9</sup> A rhodopsin-based homology model was refined by molecular dynamic simulations and validated referring to experimental data, i.e., substituted cysteine accessibility method (SCAM) results, mutational data, and structure–activity relationships (SAR) of known D3 ligands. Applying in a stepwise fashion a “hybrid” protein- and ligand-based computational approach, a virtual screening was performed. Out of 20 experimentally tested compounds, eight showed  $K_i$  values better than 1  $\mu$ M.

We have recently developed the MOBILE approach (modeling binding sites including ligand information explicitly), which models proteins by homology considering information about bound ligands as restraints, thus resulting in more relevant geometries of protein binding sites.<sup>10</sup> In a first step, ligands are docked into an ensemble of crude homology models of the target protein. In the next step, improved homology models are

\* To whom correspondence should be addressed at Institut für Pharmazeutische Chemie, Philipps-Universität Marburg, Marbacher Weg 6, 35032 Marburg, Germany. Tel: 0049 6421 2821313. Fax: 0049 6421 2828994. E-mail: klebe@mail.uni-marburg.de.

<sup>†</sup> Present address: Aventis Pharma Deutschland GmbH, DI&A Chemistry, Library Design, 65926 Frankfurt am Main, Germany.

**Table 1.** Examples of NK1 Antagonists from Diverse Structural Classes<sup>a</sup>

No	Compound	IC <sub>50</sub> [nM]	No	Compound	IC <sub>50</sub> [nM]
1	 CGP-49823	12 <sup>67</sup>	5	 0.53 <sup>68</sup>	0.53 <sup>68</sup>
2	 CP-99994	0.6 <sup>69</sup>	6	 0.21 <sup>52</sup>	0.21 <sup>52</sup>
3	 GR-203040	0.06 <sup>12</sup>	7	 L-741671	0.05 <sup>70</sup>
4	 L-709210	1.3 <sup>16</sup>	8	 1.0 <sup>71</sup>	1.0 <sup>71</sup>

<sup>a</sup> Company identification codes of the shown compounds are provided (as far as they have been named).

generated, explicitly considering the previously placed ligands by defining restraints between protein and ligand atoms. These restraints are expressed in terms of the knowledge-based distance-dependent DrugScore pair potentials, which were compiled from crystallographically determined protein–ligand complexes.<sup>11</sup> Subsequently, the most favorable models are selected by ranking the interactions between the ligands and the generated pockets using these potentials. Final models are obtained by combining the best-ranked side-chain conformers from a set of different models followed by an energy optimization of the entire complex using a common force field.

As a real-life test scenario, in the present contribution we describe the application of MOBILE to the NK1 receptor. The quality of the NK1 receptor model will be validated, and, thus, a critical evaluation of the MOBILE approach is accomplished, by probing the ability to find novel antagonists with this homology model. This task is realized by performing a virtual screening based on the modeled receptor structure and a subsequent biochemical testing of a limited number of selected hits.

Considering the fact that G-protein-coupled receptors represent one of the most relevant classes of pharmaceutical drug targets, the present study provides a particular challenge for homology modeling with respect to structure-based drug design. This holds in particular for the NK1 receptor, as its overall sequence identity to bovine rhodopsin is only 21% and in the region of the NK1 antagonist binding pocket no homology is given. A successful application of the MOBILE procedure to the NK1 receptor would therefore open a new perspective for the discovery of novel antagonists for any member of the GPCR family.

### Data Analysis and Results

**Topographical Interaction Model for NK1 Antagonists.** Meanwhile, a variety of NK1 antagonists have been reported based on several diverse lead structures (for an overview, see ref 12). Although distinct in their chemical scaffolds, they are similar with respect to the nature of functional groups decorating these scaffolds. Table 1 gives some examples for antagonists binding with high affinity to the NK1 receptor.

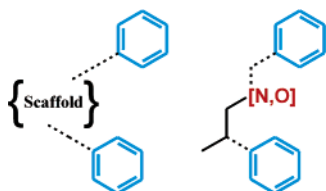


**Figure 1.** Generalized pharmacophore for nonpeptidic NK1 antagonists. Two aromatic rings are connected via various scaffolds (left). A more detailed pharmacophore contains at least one hydrogen-bond acceptor within the scaffold (right).

A generally accepted pharmacophore model for nonpeptidic NK1 antagonists is depicted in Figure 1.<sup>13</sup> It consists of at least two aromatic rings kept in fixed orientation by various scaffolds, and contains at least one hydrogen-bond acceptor. Apart from these pharmacophoric elements, a remarkable structure–activity relationship for the ligands binding with high affinity has been collected with respect to the substitution pattern at both phenyl rings. In compounds **4**, **5**, **6**, **7**, and **8** (Table 1), the “lower” phenyl ring is 3,5-bis-(trifluoromethyl)-substituted. On the other hand, compounds **2** and **3** are 2-methoxylated. The substitution pattern at this phenyl ring seems to take strong impact on binding affinity. The influence of an appropriate phenyl substitution is demonstrated by examples listed in Table 2. If the phenyl moiety of the tryptophane-

benzyl-esters is 3,5-bis-methyl-substituted (compound **10**), affinity increases at least by 6-fold. However, replacing these methyl groups by trifluoromethyls (compound **12**) results in an even 40-fold affinity increase. In another series, compound **14** exhibits 40-fold increased affinity compared to the unsubstituted phenyl ether **13**. Here, surprisingly, no remarkable affinity enhancement is observed upon replacement of the methyl by trifluoromethyl groups (compound **15**). Furthermore, the compounds in Table 2 show that affinity can be increased by substituting the exocyclic amino group. Introduction of an *N*-acetyl group at compound **10** enhances binding affinity by more than 20-fold (**11**); the same increase is observed when the carboxamidomethyl is attached to compound **15** (cf. **16**).

One of the first potent NK1 antagonists is CP-96345, discovered in 1991 by Pfizer in a high-throughput screening.<sup>14</sup> At present it is probably the best studied NK1 antagonist. The binding of several differently decorated CP-96345 derivatives was measured to obtain insight into the features responsible for binding.<sup>15–20</sup> Mutational studies and affinity measurements of such CP-96345 derivatives unraveled the key roles of Gln165<sup>4,60</sup> (according to the Ballesteros–Weinstein numbering scheme<sup>21</sup>),<sup>22</sup> His265<sup>6,52,20</sup> and His197<sup>5,39,23</sup> as binding partners for the quinuclidine antagonists.

**Table 2.** Effect of Introducing Appropriate Substituents To Increase Affinity to the NK1 Receptor

No	Compound	IC <sub>50</sub> [nM]	No	Compound	IC <sub>50</sub> [nM]
9		>10000	13		400
10		1533	14		9.3
11		67	15		10.7
12		1.6	16		0.53

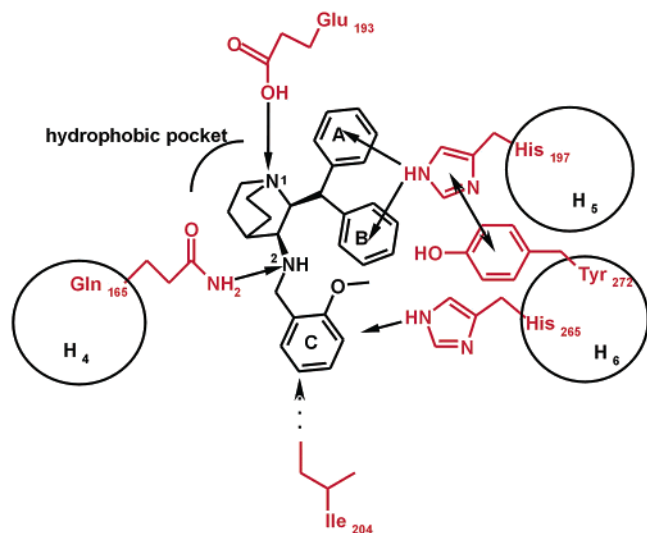


**Figure 2.** Schematic representation of the postulated NK1-receptor–ligand interactions for CP-96345. The arrows indicate proposed key interactions between the receptor and the ligand. The binding pocket falls next to the helices H<sub>4</sub> to H<sub>6</sub>.

Several groups have constructed a putative interaction model based on the skeleton of CP-96345, and the amino acid residues essential for binding could be highlighted.<sup>13,16,24–28</sup> As a consensus picture we included this information in the interaction model depicted in Figure 2. It is based on the multiple mutational data available in the literature and agrees well with the other published models. In this interaction model, Gln165<sup>4,60</sup> establishes a hydrogen bond with the exocyclic secondary amine. As high affinity binding is also obtained when this secondary amine is replaced by an oxygen, the NH<sub>2</sub> group of the terminal amide group of Gln165<sup>4,60</sup> probably acts as a donor and the ligand's NH as an acceptor. The benzhydryl group of CP-96345 performs an amino–aromatic interaction with His197<sup>5,39</sup> which itself is kept in place by an aromatic–aromatic interaction with Tyr272<sup>6,59,23</sup>. The interactions of the aromatic moiety C with Ile204<sup>5,46,29,30</sup> and His265<sup>6,52,20</sup> are apparently not specific. Instead, these residues seem to be part of a hydrophobic pocket. The aromatic moiety A occurs in several NK1 antagonists, but it is obviously not necessarily required for high affinity binding. Supposedly, it serves as conformational anchor, but does not experience any specific interactions with the receptor. Furthermore, an ionic interaction (or a charge-assisted hydrogen-bond) between the positively charged quinuclidine nitrogen and a corresponding counterpart in the receptor is possible.<sup>13</sup> A putative candidate is Glu193<sup>5,35</sup>; however, mutational data do not fully support this assumption.<sup>30,31</sup> Another explanation could be that this part of the ligand interacts with residues localized on an extracellular loop or it remains with this part exposed to the solvent. The latter hypothesis is supported by the observation that a range of diverse polar substituents hooked up to this nitrogen is well tolerated without modulating binding affinity.<sup>12</sup> A detailed study of the bioactive conformation of CP-96345 (and other antagonists) was performed by Boks et al.<sup>13</sup> They analyzed small molecule crystal structures of NK1 antagonists with respect to intermolecular interactions formed by the pharmacophoric groups with neighboring molecules in the crystal packing. The most striking

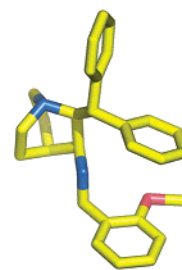


**Figure 3.** Small molecule crystal conformation of CP-96345 as observed for its *N*-methyl analogue (CSD refcode: LEWCUL).

feature is the relative orientation of the two aromatic rings with respect to each other (B and C in Figure 2). Three deviating conformers are observed in crystal structures for CP-96345 and two closely related derivatives, which exhibit distinct orientations of the aromatic ring C. In one case, a conformation with parallel orientation is observed; in the other two cases, orientations with perpendicularly oriented rings are found. In another study, a conformational search was performed by Swain et al. to identify the most favorable conformation of CP-96345;<sup>16</sup> however, no clear preference for any of the two alternative orientations could be evidenced. Modeling studies performed by Sisto et al. on a series of peptides and nonpeptides indicate that the aromatic moieties exhibit a parallel stacking with respect to each other.<sup>32</sup> This assumption is further supported by ultraviolet absorption and fluorescence measurements. In summary, these findings suggest that the conformation adopted in the crystal form of LEWCUL (CSD refcode, see Figure 3) matches best the given requirements at the binding site of the NK1 receptor.

**Generation of Protein–Ligand Complexes Using the MOBILE Approach. (A) Sequence Alignment.** The sequence alignment of bovine rhodopsin (1hxx) and the human neurokinin-1 receptor (NK1) (see Figure 4), generated automatically by PSI-BLAST<sup>33</sup> and IMPALA,<sup>34</sup> was taken analogous to a previously generated homology model of the NK1 receptor deposited in ModBase<sup>35</sup> (database accession number P25103). As apparent from the mutual alignment, the sequences are most divergent in the extracellular regions. No gaps or insertions are predicted in the transmembrane regions. However, in the antagonist binding-site region (residues marked gray in Figure 4), no matching residues are conserved.

**(B) Generation of Preliminary NK1 Receptor Models.** A set of 100 initial protein models of the NK1 receptor were generated using MODELLER6.<sup>36–38</sup> According to the algorithms implemented in MODELLER6, structures of slightly deviating geometry are subjected to the optimization step. In total, 100 different models are finally obtained, which reflect, to some extent, the conformational variability in those regions which differ in the sequence alignment. For those regions which align in the sequence space, but are matched by different amino acids (i.e., no insertion or gap), the backbone coordinates are kept close to those of the template structure, whereas the conformational space of the side-chain atoms is exhaustively sampled. The ensemble of 100 binding-site models (see Figure 5) was visually inspected in particular with respect to residues known by mutational studies to be involved in antagonist binding.<sup>14,19,29,39–50</sup> These data confirmed the



**Figure 4.** Sequence alignment of bovine rhodopsin and the NK1 receptor. All residues comprising the putative binding pocket of CP-96345 are marked in gray.

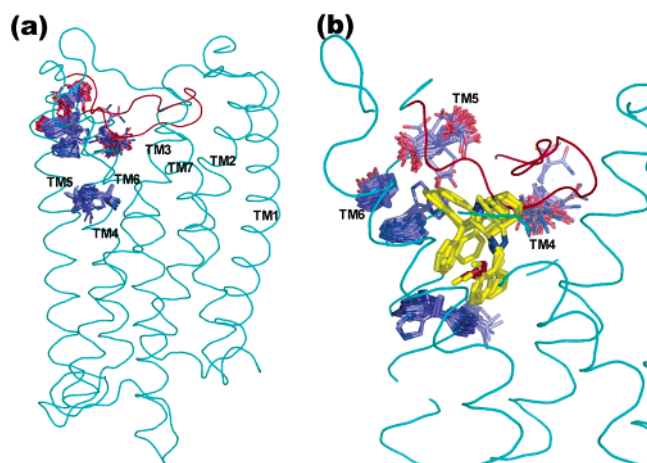


**Figure 5.** Homology models of the NK1 receptor. (a) The backbone (cyan) and an ensemble of 100 side-chain conformers involved in binding CP-96345 are shown. (b) Four docking solutions of CP-96345. Their orientations agree well with the mutational data and the proposed interaction model shown in Figure 2. The ensemble of the binding-site residues crucial for binding CP-96345 is depicted: Gln165<sup>4,60</sup>, Glu193<sup>5,35</sup>, His197<sup>5,39</sup>, Ile204<sup>5,46</sup>, His265<sup>6,52</sup>, and Tyr272<sup>6,59</sup>.

relevance of our sequence alignment: The spatial arrangement of the modeled binding-site residues is in convincing agreement with the pattern of the proposed interaction models used to describe CP-96345 binding (Figure 2). Figure 5a shows the backbone of one NK1 model together with an ensemble of orientations of those residues which are known to be involved in antagonist binding. The backbone trace of the putative  $\beta$ 4-hairpin is colored red. Since the NK1 receptor model was generated by homology, the geometry generated for this  $\beta$ 4-hairpin has been directly transferred from the bovine rhodopsin template structure. Its geometry appears unreasonable for the modeled receptor since it would clash with the antagonist binding site in the present close-up conformation. This detail of the modeled receptor clearly indicates the limitations of protein structure

prediction by homology; however, it is not crucial for the present modeling attempt since mutational studies do not offer any evidence for specific interactions of this hairpin with CP-96345.

**(C) Placing the Ligand into the Preliminary Homology Models.** In the next step, CP-96345 was docked into each single NK1 model using AutoDock 3.0<sup>51</sup> with DrugScore pair potentials serving as objective function. The E2 loop (containing the  $\beta$ 4-hairpin) as described is not crucial for the present modeling study; accordingly, it was removed from the models for the following docking procedure.

To reduce search space, CP-96345 was kept rigid during the docking into the initial homology models, simultaneously assuming that its bound conformation is similar to that observed in its crystal structure (LEWCUL)<sup>52</sup> (aromatic rings in parallel orientation, see Figure 3). Finally, the docking solutions were inspected visually, assessing whether the obtained binding modes agreed with the derived interaction model (Figure 2).<sup>13,16,24–28</sup> On the basis of these selection criteria, a total of four solutions with alternative side-chain orientations of the binding-site residues (see Figure 5b) were selected for the subsequent protein modeling step.

**(D) Generation of Refined NK1 Models Including Ligand Information and Optimization of the Modeled Protein–Ligand Complexes.** In the following step, for each of the four selected docking poses, 100 new homology models were generated using MODELLER6. According to the MOBILE approach, ligand information was now considered as additional restraint in this step of the homology modeling procedure. The 400 thus generated protein–ligand complexes were further refined. First, to each binding-site exposed amino acid a DrugScore value was assigned to describe the interaction with CP-96345. Subsequently, the best individual solutions from the different models were assembled in a combinatorial fashion, and finally the composed complex was selected which yielded the best

total DrugScore value avoiding any intramolecular clashes between individual amino acid side chains extracted from different models. In order to relax the composed model, the entire binding pocket was minimized with the MAB force field available in Moloc,<sup>53,54</sup> keeping ligand and protein residues flexible.

**Analysis of the Model. (A) Analysis of the Global Fold of the Model.** As we applied the concepts of homology modeling, the length and geometry of the transmembrane region are reproduced similarly to that in the bovine rhodopsin structure. Considering the conservation of key residues in the family of GPCRs,<sup>55</sup> there are good reasons to assume that the geometry of the transmembrane region will be conserved among these receptors. This assumption is supported by the fact that all GPCRs couple to a G-protein. Furthermore, it is likely that all GPCRs follow a similar G-protein activation mechanism. In consequence, it can be assumed that the inactive state of the NK1 receptor (as for all GPCRs) corresponds to an inactive state of bovine rhodopsin captured in the rhodopsin crystal structure which was used as template in our modeling process. As we are interested in finding antagonists, which should stabilize the NK1 receptor in its inactive state, the crystal structure of bovine rhodopsin as reference appears sufficiently relevant.

Only little confidence can be attributed to the geometry of the extracellular loops (including the  $\beta$ 4-hairpin), in contrast to the reasonably defined transmembrane region. This holds in particular true for the extracellular regions. Considering that many endogenous agonists are described to interact with the extracellular region of their receptor and recalling that these agonists represent rather diverse structures with respect to different GPCRs, it is very likely that GPCRs are very different in this region. From this point of view, it seems very unlikely that the extracellular loop regions adopt similar orientations in all GPCRs. Furthermore, it must be considered that the conformation adopted by the extracellular loops in the crystal structure of bovine rhodopsin is supposedly largely determined by crystal packing forces. However, with respect to knowledge collected by mutational studies, the antagonist binding is not directly influenced by this loop and its adopted spatial structures.

**(B) Analysis and Validation of the Active Site and Modeled Protein–Ligand Complex.** The complex of the NK1 model, including the six residues known to be crucial for CP-96345 binding, is depicted in Figure 6. The proposed interactions (as suggested by the interaction model, Figure 2) are displayed as dashed lines. As mentioned above, no sequence identity between NK1 receptor and bovine rhodopsin is given next to the assumed antagonist binding pocket. Thus, the backbone trace of the NK1 model is kept with geometry similar to the rhodopsin template, but no restrictions are imposed with respect to the orientation of the binding-site side chains. Since the NK1 model was generated and optimized to produce a binding pocket that exhibits optimal interactions with CP-96345, the arrangement of these side chains is predominantly determined according to the docked binding mode of this ligand. The finally achieved spatial arrangement of the binding-site residues agrees well with the topographic interaction

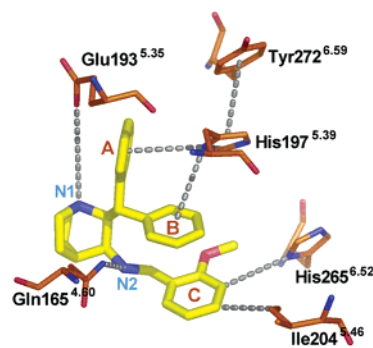


**Figure 6.** Modeled complex of the NK1 receptor with CP-96345. The dashed lines indicate the key interactions of the proposed interaction model depicted in Figure 2.

model depicted in Figure 2: All residues known to be crucial for CP-96345 binding are in specific contact with the ligand in our model. Retrospectively, this fact confirms the relevance of the assumed sequence alignment. As indicated by the mutational data, the most important interaction between NK1 receptor and antagonists is the hydrogen bond formed between the terminal  $\text{NH}_2$  amide of Gln165<sup>4,60</sup> and a hydrogen-bond acceptor group of the antagonist. This interaction is well reproduced by our model and amounts to a distance of 3.21 Å (see Figure 6). Our model also reproduces the suggested amino–aromatic interactions,<sup>23</sup> which are established between the aromatic rings A and B and His197.<sup>5,39</sup> This latter residue is fixed in space by an aromatic–aromatic interaction with Tyr272<sup>6,59</sup>. The role of His265<sup>6,52</sup> and Ile204<sup>5,46</sup> and their interactions with the ligand remain unclear. In agreement with mutational data, instead of specific interactions, hydrophobic contacts between the aromatic moiety C and His265<sup>6,52</sup>/Ile204<sup>5,46</sup> are established. A possible ionic interaction between the nitrogen N1 and a corresponding protein partner is not fully evidenced, neither by the mutational data nor by our model (the distance to the Glu193<sup>5,35</sup>-carboxy oxygen amounts to 5.58 Å). The mutational data show that a slight change in affinity is detected when Glu193<sup>5,35</sup> is mutated to Ala or His;<sup>30,31</sup> however, as this decrease is not highly significant (less than 3-fold and 7-fold), and the ionic interaction cannot be reproduced by our model, N1 is possibly exposed to solvent and does not interact directly with Glu193<sup>5,35</sup> or another neighboring amino acid.

As indicated above, it is unlikely that the orientation of the  $\beta$ 4-hairpin adopts a similar geometry as in bovine rhodopsin. Indeed, in our modeled complex, CP-96345 would clash with the  $\beta$ 4-hairpin if it would adopt the same orientation (see Figure 5b). It was shown by Cavasotto et al. that retinal can be docked accurately into the bovine rhodopsin pocket even if the N-terminus, C-terminus, and extracellular (including the  $\beta$ 4-hairpin) and intracellular loops are removed.<sup>5</sup> Even though retinal is in contact with the  $\beta$ 4-hairpin in the rhodopsin crystal structure, the majority of the ligand is deeply buried and its binding is sufficiently determined by contacts established to the transmembrane part of the receptor. This observation suggests that similar conditions are given for our NK1 receptor model that allow identification of novel ligands. This assumption is further supported by the fact that mutations within the  $\beta$ 4-hairpin of the NK1 receptor did not take substantial

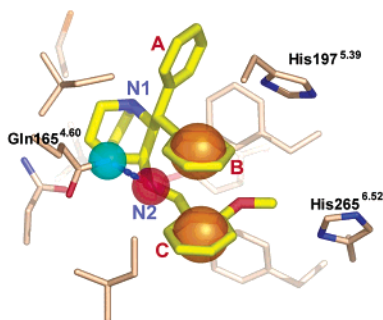


**Figure 7.** Structure-based pharmacophore hypothesis. The H-bond interaction between the  $\text{NH}_2$  of the terminal amide group of Gln165<sup>4.60</sup> (cyan sphere) and a corresponding H-bond acceptor (red) is considered essential for all NK1 antagonists. The sites for aromatic moieties are indicated by yellow spheres.

influence on the binding of CP-96345. From a pragmatic point of view, a possible option for structure-based drug design is to fully neglect this region in the search of new antagonists. This, however, could provoke docking solutions for ligands that are artificially oriented into this unoccupied region. Therefore, to restrict the binding pocket to some degree, however simultaneously to avoid specific interactions to the putative binding site of CP-96345, we manually placed the  $\beta$ 4-hairpin loop in a somewhat distant region. Subsequently, the corresponding residues were relaxed using the AMBER force field<sup>56</sup> to avoid an unreasonable geometry. In the following virtual screening procedure, the relevance of the docking modes produced for candidate ligands was evidenced not solely by evaluating their interaction geometry but in addition by considering their spatial similarity with known NK1 antagonists (see Table 1). To further assess the relevance of the produced model, we examined its ability to accommodate these known reference NK1 antagonists by docking them into the modeled NK1 receptor binding site using FlexX-Pharm.<sup>57</sup> In all cases, reasonable orientations were obtained.

**Generation of a Composite Protein- and Ligand-Based Pharmacophore.** On the basis of the modeled NK1–CP-96345 complex, a structure-based pharmacophore hypothesis has been generated considering the mutational data from literature and the features common to all considered known NK1 antagonists. This pharmacophore model is characterized by the following three features (see Figures 2 and 7):

1. A hydrogen bond between the terminal amide group of Gln165<sup>4.60</sup> and a corresponding acceptor of the ligand (N2 in CP-96345). The importance of this hydrogen bond, as indicated by Fong et al.,<sup>22</sup> is best demonstrated by the observation that, upon replacement of N2 in CP-96345 by a carbon atom, a dramatic loss in affinity (0.52 to >32000 nM) is detected.<sup>18</sup>

2. The aromatic moiety B interacts with His197<sup>5.39</sup> via amino–aromatic interactions.<sup>23</sup>

3. A second aromatic group (C) is required that falls next to His265<sup>6.52</sup><sup>20</sup> and Ile204<sup>5.46, 29, 30</sup>. Obviously it does not form specific interactions to His265<sup>6.52</sup>, but favorable interactions are observed for CP-96345 analogues that show substituents at ring C. Although the detailed nature of these interactions is not clear, the analysis of known NK1 antagonists reveals that an aromatic moiety C is essential for high-affinity binding to the NK1 receptor.

**Virtual Screening.** In the present study, about 827000 candidate molecules, assembled from seven different databases, were screened to retrieve putative NK1 antagonists. The same set of compounds was previously studied in our group to search tRNA-guanine transglycosylase (TGT) inhibitors.<sup>58</sup> Similar to the studies of Brenk et al.<sup>58</sup> and Grüneberg et al.,<sup>59</sup> the screening has been performed in a stepwise fashion using Selector, Unity, and FlexX-Pharm and considered several hierarchical filters of increasing complexity with respect to their computational requirements. The initial step, a rather unspecific and target-independent filter, was already applied by Brenk et al.: Only compounds with up to seven rotatable bonds and a molecular mass of less than 450 Da have been considered. The restrictions were applied to retrieve putative candidates small enough to allow for further optimization, originally defined as “leadlike” hits.<sup>60,61</sup> Furthermore, highly flexible ligands are avoided as they possibly (1) experience reduced binding affinity due to entropic considerations and (2) increase the complexity and thus reduce the success rate of the attempted 3D searches. A further rationale to restrict flexibility arises from the observation that the chances to produce reliable docking solutions diminishes with an increasing number of rotatable bonds of the candidate molecules. Almost 50% of the initial database entries were discarded by this filter.

In a second step, a topological filter was applied according to the pharmacophore requirements given in Figure 1. Only candidate molecules comprising at least (a) two phenyl rings and (b) one hydrogen-bond acceptor were further considered. This reduced the list of prospective compounds to about 16% of the initial set. In the following step, the combined 3D protein- and ligand-based pharmacophore hypothesis (Figure 7) was used to constrain the mutual spatial arrangement of the aromatic rings and the hydrogen-bond acceptor. In a fourth step, receptor information was explicitly included by restraining the directionality of the hydrogen bond (to interact with the terminal amino group of Gln165<sup>4.60</sup>) and by considering excluded volume constraints. The number of hits in agreement with this filter amounted to 11109 compounds. Accordingly, the hierarchical filtering procedure reduced the databases to 1.34% of their original size (Table 3). The remaining compounds were docked into the binding site of our NK1 homology model. To retrieve only hits that satisfy our 3D pharmacophore model, we used FlexX-Pharm for docking, which allows the incorporation of constraints derived from a pharmacophore hypothesis. Accordingly, the following features were included (Figure 7): The phenyl ring B was defined as base fragment for the incremental construction algorithm used in the docking procedure. This was accomplished using the phenyl ring coordinates of the initially modeled orientation of CP-96345 applying the mapref command in FlexX. The hydrogen bond formed to the amide  $\text{NH}_2$  of Gln165<sup>4.60</sup> by a corresponding hydrogen-bond acceptor of the ligand was constrained as being essential. The orientation of the additional aromatic ring (C) was not constrained in order to formulate a not too stringent search query by FlexX-Pharm that would allow only for very little variations in the molecular skeletons. Instead, the protein environment has been used as further con-

**Table 3.** Statistical Overview of the Results from Sequential Application of the Series of Hierarchical Filters on the Seven Considered Databases<sup>a</sup>

filter step	ACD		AMBINTER		AEGC		AEPC	
	no. of compds <sup>a</sup>	%	no. of compds <sup>a</sup>	%	no. of compds <sup>a</sup>	%	no. of compds <sup>a</sup>	%
1. rotatable bonds/MW	215212	100.00	115815	100.00	182485	100.00	44549	100.00
2. requested no. of hydrophobic, donor, and acceptor properties	135502	62.96	59877	51.70	91677	50.24	9417	21.14
3. pharmacophore hypothesis	30878	19.34	19764	17.07	36302	19.89	2740	6.15
4. excluded volumes	8645	4.02	5353	4.62	10534	5.77	1018	2.29
	3084	1.43	1510	1.30	2998	1.64	334	0.75
filter step	ChemStar		IBS		LEADQUEST		Σ	
	no. of compds <sup>a</sup>	%	no. of compds <sup>a</sup>	%	no. of compds <sup>a</sup>	%	no. of compds <sup>a</sup>	%
1. rotatable bonds/MW	57927	100.00	158942	100.00	52002	100.00	826952	100.00
2. requested no. of hydrophobic, donor, and acceptor properties	28712	49.57	76321	48.02	18231	35.04	419747	50.76
3. pharmacophore hypothesis	11229	19.38	24571	15.46	6483	12.47	131967	15.95
4. excluded volumes	3547	6.12	5463	3.44	2144	4.12	36704	4.44
	1226	2.12	1362	0.86	595	1.14	11109	1.34

<sup>a</sup> Release dates: ACD, 2000; AMBINTER, 2001; AEGC, AEPC, ChemStar, and IBS, 2001; Leadquest, 2000.

straint. All docking solutions were scored with DrugScore.<sup>11</sup> Previous experience has shown that DrugScore scales with the surface portion of the ligands being in contact with the protein. We therefore normalized the score with respect to the number of non-hydrogen atoms of each placed candidate ligand.<sup>62</sup>

For the 1000 best-ranked ligands, the optimal docking solutions were minimized with the MAB force field available in Moloc<sup>53,54</sup> keeping the ligand and the binding pocket (i.e., all residues within 6 Å around the ligand) flexible.

The purpose of this procedure was (1) to optimize the local interactions and (2) to account for protein flexibility induced by ligand binding. The obtained minimized solutions were visually screened in order to reject those poses which did not show the aromatic ring C in parallel orientation to ring B as depicted in Figure 7. The remaining ca. 250 solutions were inspected more carefully considering the following aspects. Ideally, the selection of virtual screening hits should be solely based on the ranking of the scoring function used to examine the interaction geometry of the docked ligands. However, many binding features in the protein–ligand interface are yet not fully understood and certain observations cannot be reproduced adequately enough by current scoring functions. Furthermore, it has been shown that the performance of a scoring function possibly depends on binding characteristics present in a particular protein–ligand interface, such as hydrophobicity, hydrophilicity, dominance of electrostatic/H-bond properties, etc.<sup>63,64</sup> In addition, general observations from quantitative structure–activity relationships prompted us to carefully inspect the best hits from the virtual screening with special regard to the following characteristics:

1. An amino–aromatic interaction should be present between His197<sup>5,39</sup> and the aromatic moiety B. This type of interaction is not yet parametrized and validated in the current scoring functions.

2. Most scoring functions do not consider intramolecular interactions when evaluating protein–ligand interactions, in particular aromatic–aromatic interactions. The described  $\pi$ – $\pi$  stacking, as observed between

the aromatic moieties B and C, seems to have a favorable impact on binding; thus its occurrence has been requested.

3. As the binding pocket and most interactions between the NK1 receptor and its antagonists are mainly hydrophobic, the hydrogen bond between the NH<sub>2</sub> group of Gln165<sup>4,60</sup> and a corresponding ligand acceptor was carefully analyzed. This interaction seems to be of utmost importance: its loss parallels a dramatic reduction in binding affinity.<sup>18</sup> This is probably impossible to consider quantitatively correctly in any scoring function.

4. As the model is not reliable next to the region of the  $\beta$ 4-hairpin, parts of the candidate molecules placed into this region were evaluated with respect to a given similarity with known NK1 antagonists. We furthermore focused on putative hits with a limited number of rotatable bonds to avoid entropically unfavorable binding due to pronounced conformational immobilization.

Applying these criteria in a thorough visual inspection of the retrieved candidates, the seven compounds shown in Figure 8 were selected for biochemical testing.

**Testing for Binding.** Affinity measurements were kindly performed by AstraZeneca. As assay a radioligand binding assay on whole CHO (Chinese hamster ovary) cells (with substance P as radioligand) has been performed. The assay was adjusted to be only sensitive to detect ligands of at least 1  $\mu$ M potency. Any weaker binding beyond this rather stringent limit cannot be detected. Out of the seven selected compounds, one (ASN-1377642) shows 0.25  $\mu$ M affinity. ASN-1377642 agrees well with our 3-dimensional pharmacophore hypothesis. Comparing ASN-1377642 and CP-96345 in their docked binding modes reveals that the aromatic moieties and the position of the hydrogen-bond acceptors superimpose well. Even the postulated amino–aromatic interaction between His197<sup>5,39</sup> and the aromatic ring is matched similarly to CP-96345. The hydrogen bond to the NH<sub>2</sub> group of Gln165<sup>4,60</sup> is established via the ligand's peptide carbonyl oxygen (see Figure 9). Furthermore, the sulfur of the thioether group could be involved as an additional hydrogen-bond acceptor. The peptide bond rigidifies the ligand's skeleton and has



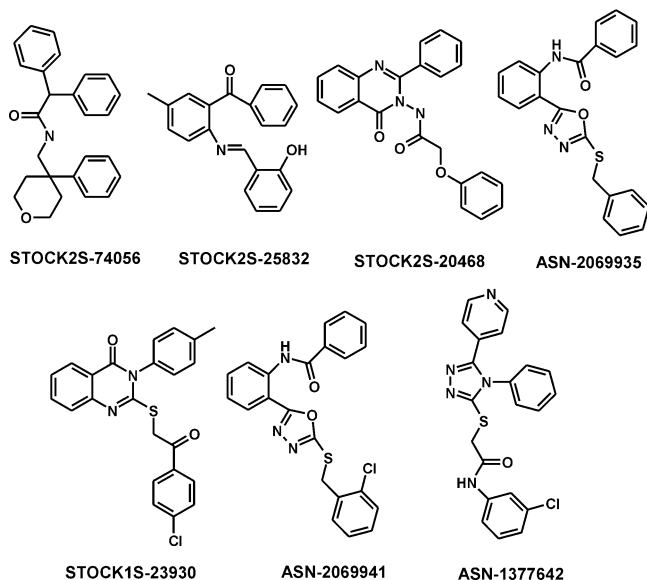


**Figure 8.** List of compounds that were tested for inhibition against the NK1 receptor. ASN-1377642 showed 251 nM affinity. The compounds were purchased from IBS (STOCK2S-74056, STOCK2S-25832, STOCK2S-20468, STOCK1S-23930) and AEPC (ASN-2069935, ASN-2069941, ASN-1377642).

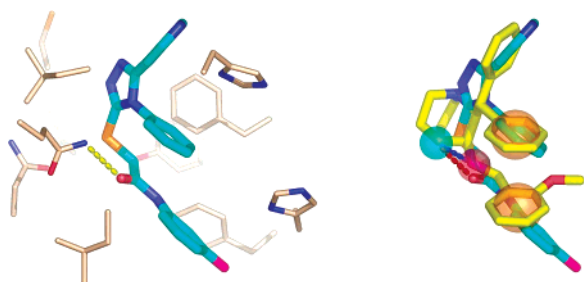


**Figure 9.** Modeled binding mode of ASN-1377642, which was identified as novel submicromolar NK1 antagonist by virtual screening. The orientation with respect to the modeled binding pocket is shown (left). On the right, a superimposition of ASN-1377642 with the known NK1 antagonist CP-96345 is shown.

possibly a favorable impact on the entropic contribution to binding. Considering the docked binding mode of ASN-1377642, both aromatic moieties (B and C in the pharmacophore model) exhibit a parallel arrangement; however, they are shifted with respect to each other in a way that they do not establish a  $\pi$ - $\pi$ -stacking interaction. Instead, according to our model, the aromatic ring B stacks upon the  $\pi$ -face of the peptide bond. In addition, ASN-1377642 exhibits the aromatic moiety A (Figure 7) that is present in several of the known NK1 antagonists. However, it is obviously not mandatory for high affinity binding. As mentioned before, it probably serves as a conformational anchor, but does not perform any specific interaction with the receptor. Interestingly enough, besides STOCK2S-74056, ASN-1377642 is the only one out of the seven compounds selected for testing that possesses this moiety.

## Discussion and Conclusions

In this contribution, we present a strategy for the computer screening of large compound libraries targeted for the NK1 receptor. This receptor belongs to the family of G-protein coupled receptors, which represents one of the most important pharmaceutical drug target classes.

Our approach, which can in principle be applied to any member of the GPCR family in its inactive state, is based on a homology model generated from the crystal structure of bovine rhodopsin as structural template. The NK1 model was constructed explicitly considering ligand information via our recently developed MOBILE approach (modeling binding sites including ligand information explicitly).<sup>10</sup> The model was validated by reproducing experimental information such as mutational data and corresponding affinity data of known ligands. It was successfully used to screen seven databases containing in total about 827000 compounds. Docking retrieved one novel compound (out of seven hits selected for biochemical testing) that binds to the receptor with submicromolar affinity. Any possible weaker binding of the other selected hits could not be registered due to a detection limit of approximately 1  $\mu$ M under the applied assay conditions. Similar virtual screening protocols have previously been performed in our group to discover novel inhibitors for the tRNA-guanine transglycosylase (TGT),<sup>58</sup> carbonic anhydrase II,<sup>59</sup> and aldose reductase.<sup>65</sup> These studies were based on well-resolved crystal structures of several protein-ligand complexes. Due to the limited accuracy of the structural reference used in the present study, the applied search strategy has been modified and certain steps have been adopted to cope with potential structural deficiencies of our homology model.

We started with the generation of preliminary protein models. After subsequent docking into these crude models, a refined protein-ligand complex was generated considering the placed ligands. The model was finally checked for consistency with mutational and known ligand-binding data. In the following, it served as a platform to generate a composed protein- and ligand-structure-based pharmacophore hypothesis and as structural reference for database searching. Thus, in our approach, ligand information was not only explicitly included in the protein modeling step but also considered in the screening and scoring procedure. For the initial screening only those compounds out of 827000 database entries were selected that agreed to simple 2D pharmacophore features established as minimal prerequisite according to the analysis of the binding requirement of known NK1 antagonists. In subsequent steps, ligand information was taken into account by applying 3D pharmacophore features derived from the analysis of the putative binding mode of the ligand CP-96345, docked into our NK1 model. In contrast to the approach followed by Brenk et al. or Grüneberg et al., these pharmacophore features were also used to constrain the docking protocol within FlexX-Pharm. As a further difference from the above-mentioned studies, the entire protein-ligand complexes were minimized using the MAB force field to consider possible adaptations of the protein induced by ligand binding and to account at least to some extent for potential structural deficiencies of our model. Finally, the binding modes obtained by docking were carefully inspected to assess how well the candidate ligands matched the pharmacophore query and local interaction features known to occur in active NK1 antagonists. Considering the fact that CP-96345 and the discovered hit ASN-1377642 correspond with respect to their pharmacophoric features, but differ

with respect to their molecular skeletons, we believe that this hit could not be retrieved as a top ranking hit using a solely ligand-based or a solely protein-based screening strategy. The prime focus of this study was to demonstrate that ligand-supported homology modeling of a GPCR can be accomplished using MOBILE with an accuracy sufficient to perform a subsequent virtual screening.

The newly discovered lead ASN-1377642 has yet not been further optimized. Possibly, as outlined above, a remarkable affinity increase could be achieved by introduction of a 3,5-bis(trifluoromethyl) substitution at the aromatic moiety C. Swain et al. suggested as possible explanation of this enhancement a stabilized arrangement of both aromatic moieties B and C with respect to each other or the experience of favorable lipophilic contacts with His265<sup>6,52,16</sup>. Further lead optimization of ASN-1377642 could be attempted by an appropriate substitution of one of the nitrogen atoms at the triazole ring, e.g., through the attachment of an *N*-acetyl or carboxamidomethyl group (cf. examples in Table 2).

The applied procedure of combining information about structure–activity relationships of known bioactive ligands and the spatial structure of a homologous protein (here: bovine rhodopsin), along with mutational data, provides new perspectives to drug discovery of GPCR ligands. Remarkably enough, the global sequence identity between bovine rhodopsin and the NK1 receptor is only 21%. Considering the transmembrane region only, the identity increases to 27%; however, regarding the modeled binding site of CP-96345 only, no sequence identity is given. These facts point to uncertainties in modeling GPCR pockets on the basis of the bovine rhodopsin structure. To allow for the prediction of relevant binding site geometries by homology, a preservation of the backbone geometry is necessary. The fact that all GPCRs share highly conserved key residues in each helix<sup>55</sup> suggests such structural conservation; however, experimental evidence (e.g., the crystal structure of another GPCR) is still missing. Usually, if sequence identity falls beyond 35%, the accuracy of any produced homology model is considered insufficient to allow for virtual screening and docking of small ligands.<sup>66</sup> In light of this nonconserved antagonist binding site among NK1 receptor and bovine rhodopsin it is even more remarkable that our MOBILE approach produced a binding-site geometry reliable and relevant enough to discover a submicromolar antagonist via structure-based screening.

However, it must be noted that precise affinity prediction is not possible with our model. To a certain extent, this is due to shortcomings of the currently available docking programs and scoring functions. Further limitations probably arise from the fact that the structural reference for affinity prediction is only given by a crude homology model. In particular, toward the  $\beta$ -hairpin, our model is very crude and approximate. It thus cannot correctly reflect the native configuration of the protein and appropriately describe contributions to binding affinity in this area.

An important binding determinant is the H-bond formed to Gln165<sup>4,60</sup>. Mutational and ligand structure–activity data provide clear evidence that Gln165<sup>4,60</sup> acts

as a H-bond donor. It could furthermore serve as H-bond acceptor, depending on the side-chain orientation of the terminal amide group and the binding partner group in the ligand. This would have consequences for the definition of the pharmacophore model used to specify the search queries. In our search, we requested an acceptor functionality in putative ligands. An alternative pharmacophore model could demand either an acceptor or donor site at this position and would extend the scope for searches of putative NK1 antagonists. Furthermore, in the 3D pharmacophore model, the mutual arrangement of the aromatic rings was assumed to exhibit parallel orientation analogous to the geometry observed in the small molecule crystal structure LEWCUL and further evidenced by ultraviolet absorption and fluorescence measurements in the bound state.<sup>32</sup> Nevertheless, two other small molecule crystal structures indicate that a perpendicular edge-to-face arrangement of these aromatic moieties also corresponds to a low-energy conformer. Accordingly, it cannot be excluded that the latter geometry could also correspond to the bound arrangement at the receptor site. Neither the available mutational data nor local contacts formed by both aromatic rings with adjacent protein residues favors one of these arrangements. Furthermore, it has to be mentioned that originally 15 compounds were selected for biochemical testing. Due to inaccessibility or delivery problems of the commercial suppliers, we could only obtain half of the requested compounds (7). The affinity determination was performed using an assay with a detection limit beyond 1  $\mu$ M affinity. Testing at higher concentration could not be performed under the setup available to us. For the present feasibility study it would be highly desirable to obtain detailed binding data for perhaps the first 100 hits, which would allow for statistics on the success rates of our approach. However, to demonstrate that homology modeling using MOBILE is capable to produce models of relevance for structure-based virtual screening, the discovered hit which is in full agreement with the search hypothesis is in our opinion a remarkable and convincing result.

**Acknowledgment.** The authors are grateful to Dr. Arne Svensson (AstraZeneca, Mölndal, Sweden) for determining the binding affinities of the seven test compounds described in this report. We also thank Dr. R. Brenk (University of Marburg) for providing the chemical databases used for the virtual screening. Furthermore we would like to express our thanks to Tripos (Munich, Germany) and BioSolveIT for making their software tools available to us. 3D-coordinates of the homology model can be obtained from the authors upon request.

## References

- (1) Klabunde, T.; Hessler, G. Drug design strategies for targeting G-protein-coupled receptors. *ChemBioChem* **2002**, *3*, 928–944.
- (2) Palczewski, K.; Kumasaka, T.; Hori, T.; Behnke, C. A.; Motoshima, H.; et al. Crystal structure of rhodopsin: A G protein-coupled receptor. *Science* **2000**, *289*, 739–745.
- (3) Flohr, S.; Kurz, M.; Kostenis, E.; Brkovich, A.; Fournier, A.; et al. Identification of nonpeptidic urotensin II receptor antagonists by virtual screening based on a pharmacophore model derived from structure–activity relationships and nuclear magnetic resonance studies on urotensin II. *J. Med. Chem.* **2002**, *45*, 1799–1805.

- (4) Marriott, D. P.; Dougall, I. G.; Meghani, P.; Liu, Y. J.; Flower, D. R. Lead generation using pharmacophore mapping and three-dimensional database searching: application to muscarinic M(3) receptor antagonists. *J. Med. Chem.* **1999**, *42*, 3210–3216.
- (5) Cavasotto, C. N.; Orry, A. J.; Abagyan, R. A. Structure-based identification of binding sites, native ligands and potential inhibitors for G-protein coupled receptors. *Proteins* **2003**, *51*, 423–433.
- (6) Berkhout, T. A.; Blaney, F. E.; Bridges, A. M.; Cooper, D. G.; Forbes, I. T.; et al. CCR2: characterization of the antagonist binding site from a combined receptor modeling/mutagenesis approach. *J. Med. Chem.* **2003**, *46*, 4070–4086.
- (7) Bissantz, C.; Bernard, P.; Hibert, M.; Rognan, D. Protein-based virtual screening of chemical databases. II. Are homology models of G-Protein Coupled Receptors suitable targets? *Proteins* **2003**, *50*, 5–25.
- (8) Becker, O. M.; Shacham, S.; Marantz, Y.; Noiman, S. Modeling the 3D structure of GPCRs: advances and application to drug discovery. *Curr. Opin. Drug Discovery Dev.* **2003**, *6*, 353–361.
- (9) Varady, J.; Wu, X.; Fang, X.; Min, J.; Hu, Z.; et al. Molecular modeling of the three-dimensional structure of dopamine 3 (D3) subtype receptor: discovery of novel and potent D3 ligands through a hybrid pharmacophore- and structure-based database searching approach. *J. Med. Chem.* **2003**, *46*, 4377–4392.
- (10) Evers, A.; Gohlke, H.; Klebe, G. Ligand-supported Homology Modelling of Protein Binding-sites using Knowledge-based Potentials. *J. Mol. Biol.* **2003**, *334*, 327–345.
- (11) Gohlke, H.; Hendlich, M.; Klebe, G. Knowledge-based scoring function to predict protein-ligand interactions. *J. Mol. Biol.* **2000**, *295*, 337–356.
- (12) Gardner, C. J.; Twissel, D. J.; Dale, T. J.; Gale, J. D.; Jordan, C. C.; et al. The Broad-Spectrum Antiemetic Activity of the Novel Non-peptide Tachykinin NK1 Receptor Antagonist GR203040. *Br. J. Pharmacol.* **1995**, *116*, 3158–3163.
- (13) Boks, G. J.; Tollenaere, J. P.; Kroon, J. Possible ligand-receptor interactions for NK1 antagonists as observed in their crystal structures. *Bioorg. Med. Chem.* **1997**, *5*, 535–547.
- (14) Snider, R. M.; Constantine, J. W.; Lowe, J. A., 3rd; Longo, K. P.; Lebel, W. S.; et al. A potent nonpeptide antagonist of the substance P (NK1) receptor. *Science* **1991**, *251*, 435–437.
- (15) Seward, E. M.; Owen, S. N.; Sabin, V.; Swain, C. J.; Cascieri, M. A.; et al. Quinuclidine-Based NK-1 Antagonists I: 3-Benzyl-oxy-1-Azabicyclo[2.2.2]octanes. *Bioorg. Med. Chem. Lett.* **1993**, *3*, 1361–1366.
- (16) Swain, C. J.; Seward, E. M.; Cascieri, M. A.; Fong, T. M.; Herbert, R.; et al. Identification of a series of 3-(benzyloxy)-1-azabicyclo[2.2.2]octane human NK1 antagonists. *J. Med. Chem.* **1995**, *38*, 4793–4805.
- (17) Lowe, J. A., III; Drozda, S. E.; McLean, S.; Bryce, D. K.; Crawford, R. T.; et al. Aza-tricyclic substance P antagonists. *J. Med. Chem.* **1994**, *37*, 2831–2840.
- (18) Lowe, J. A., III; Drozda, S. E.; Snider, R. M.; Longo, K. P.; Zorn, S. H.; et al. The discovery of (2*S*,3*S*)-*cis*-2-(diphenylmethyl)-*N*-[(2-methoxyphenyl)methyl]-1-azabicyclo[2.2.2]octan-3-amine as a novel, nonpeptide substance P antagonist. *J. Med. Chem.* **1992**, *35*, 2591–2600.
- (19) Fong, T. M.; Huang, R. R.; Yu, H.; Strader, C. D. Mapping the ligand binding site of the NK-1 receptor. *Regul. Pept.* **1993**, *46*, 43–48.
- (20) Fong, T. M.; Yu, H.; Cascieri, M. A.; Underwood, D.; Swain, C. J.; et al. The role of histidine 265 in antagonist binding to the neurokinin-1 receptor. *J. Biol. Chem.* **1994**, *269*, 2728–2732.
- (21) Ballesteros, J. A.; Weinstein, H. Integrated methods for the construction of three-dimensional models and computational probing of structure-function relations in G protein-coupled receptors. *Methods Neurosci.* **1995**, *25*, 366–428.
- (22) Fong, T. M.; Yu, H.; Cascieri, M. A.; Underwood, D.; Swain, C. J.; et al. Interaction of glutamine 165 in the fourth transmembrane segment of the human neurokinin-1 receptor with quinuclidine antagonists. *J. Biol. Chem.* **1994**, *269*, 14957–14961.
- (23) Fong, T. M.; Cascieri, M. A.; Yu, H.; Bansal, A.; Swain, C.; et al. Amino-aromatic interaction between histidine 197 of the neurokinin-1 receptor and CP 96345. *Nature* **1993**, *362*, 350–353.
- (24) Elliott, J. M.; Broughton, H.; Cascieri, M. A.; Chicchi, G.; Huscroft, I. T.; et al. Serine derived NK1 antagonists. 2: A pharmacophore model for arylsulfonamide binding. *Bioorg. Med. Chem. Lett.* **1998**, *8*, 1851–1856.
- (25) Elliott, J. M.; Cascieri, M. A.; Chicchi, G.; Davies, S.; Kelleher, F. J.; et al. Serine derived NK1 antagonists. 1: The effect of modifications to the serine substituents. *Bioorg. Med. Chem. Lett.* **1998**, *8*, 1845–1850.
- (26) Takeuchi, Y.; Shands, E. F. B.; Beusen, D. D.; Marshall, G. R. Derivation of a three-dimensional pharmacophore model of substance P antagonists bound to the neurokinin-1 receptor. *J. Med. Chem.* **1998**, *41*, 3609–3623.
- (27) Jacoby, E.; Boudon, A.; Kucharczyk, N.; Michel, A.; Fauchere, J. L. A structural rationale for the design of water soluble peptide-derived neurokinin-1 antagonists. *J. Recept. Signal Transduction Res.* **1997**, *17*, 855–873.
- (28) Vedani, A.; Briem, H.; Dobler, M.; Dollinger, H.; McMasters, D. R. Multiple-conformation and protonation-state representation in 4D-QSAR: the neurokinin-1 receptor system. *J. Med. Chem.* **2000**, *43*, 4416–4427.
- (29) Holst, B.; Zoffmann, S.; Elling, C. E.; Hjorth, S. A.; Schwartz, T. W. Steric hindrance mutagenesis versus alanine scan in mapping of ligand binding sites in the tachykinin NK1 receptor. *Mol. Pharmacol.* **1998**, *53*, 166–175.
- (30) Greenfeder, S.; Cheewatrakoolpong, B.; Anthes, J.; Billah, M.; Egan, R. W.; et al. Two related neurokinin-1 receptor antagonists have overlapping but different binding sites. *Bioorg. Med. Chem.* **1998**, *6*, 189–194.
- (31) Elling, C. E.; Nielsen, S. M.; Schwartz, T. W. Conversion of antagonist-binding site to metal-ion site in the tachykinin NK-1 receptor. *Nature* **1995**, *374*, 74–77.
- (32) Sisto, A.; Bonelli, F.; Centini, F.; Fincham, C. I.; Potier, E.; et al. Synthesis and biological evaluation of novel NK-1 tachykinin receptor antagonists: the use of cycloalkyl amino acids as a template. *Biopolymers* **1995**, *36*, 511–524.
- (33) Altschul, S. F.; Madden, T. L.; Schaffer, A. A.; Zhang, J.; Zhang, Z.; et al. Gapped BLAST and PSI-BLAST: a new generation of protein database search programs. *Nucleic Acids Res.* **1997**, *25*, 3389–3402.
- (34) Schaffer, A. A.; Wolf, Y. I.; Ponting, C. P.; Koonin, E. V.; Aravind, L.; et al. IMPALA: matching a protein sequence against a collection of PSI-BLAST-constructed position-specific score matrices. *Bioinformatics* **1999**, *15*, 1000–1011.
- (35) Pieper, U.; Eswar, N.; Stuart, A. C.; Ilyin, V. A.; Sali, A. MODBASE, a database of annotated comparative protein structure models. *Nucleic Acids Res.* **2002**, *30*, 255–259.
- (36) Marti-Renom, M. A.; Stuart, A. C.; Fiser, A.; Sanchez, R.; Melo, F.; et al. Comparative protein structure modeling of genes and genomes. *Annu. Rev. Biophys. Biomol. Struct.* **2000**, *29*, 291–325.
- (37) Sali, A.; Blundell, T. L. Comparative protein modelling by satisfaction of spatial restraints. *J. Mol. Biol.* **1993**, *234*, 779–815.
- (38) Fiser, A.; Do, R. K.; Sali, A. Modeling of loops in protein structures. *Protein Sci.* **2000**, *9*, 1753–1773.
- (39) Garret, C.; Carruette, A.; Fardin, V.; Moussaoui, S.; Peyronel, J. F.; et al. Pharmacological properties of a potent and selective nonpeptide substance P antagonist. *Proc. Natl. Acad. Sci. U.S.A.* **1991**, *88*, 10208–10212.
- (40) Cascieri, M. A.; Huang, R. R.; Fong, T. M.; Cheung, A. H.; Sadowski, S.; et al. Determination of the amino acid residues in substance P conferring selectivity and specificity for the rat neurokinin receptors. *Mol. Pharmacol.* **1992**, *41*, 1096–1099.
- (41) Fong, T. M.; Huang, R. R.; Strader, C. D. Localization of agonist and antagonist binding domains of the human neurokinin-1 receptor. *J. Biol. Chem.* **1992**, *267*, 25664–25667.
- (42) Gether, U.; Johansen, T. E.; Snider, R. M.; Lowe, J. A., 3rd; Nakanishi, S.; et al. Different binding epitopes on the NK1 receptor for substance P and non-peptide antagonist. *Nature* **1993**, *362*, 345–348.
- (43) Gether, U.; Johansen, T. E.; Snider, R. M.; Lowe, J. A., 3rd; Emonds-Alt, X.; et al. Binding epitopes for peptide and non-peptide ligands on the NK1 (substance P) receptor. *Regul. Pept.* **1993**, *46*, 49–58.
- (44) Gether, U.; Nilsson, L.; Lowe, J. A., 3rd; Schwartz, T. W. Specific residues at the top of transmembrane segment V and VI of the neurokinin-1 receptor involved in binding of the nonpeptide antagonist CP 96,345 [corrected]. *J. Biol. Chem.* **1994**, *269*, 23959–23964.
- (45) Gether, U.; Yokota, Y.; Emonds-Alt, X.; Breliere, J. C.; Lowe, J. A., 3rd et al. Two nonpeptide tachykinin antagonists act through epitopes on corresponding segments of the NK1 and NK2 receptors. *Proc. Natl. Acad. Sci. U.S.A.* **1993**, *90*, 6194–6198.
- (46) Gether, U.; Emonds-Alt, X.; Breliere, J. C.; Fujii, T.; Hagiwara, D.; et al. Evidence for a common molecular mode of action for chemically distinct nonpeptide antagonists at the neurokinin-1 (substance P) receptor. *Mol. Pharmacol.* **1994**, *45*, 500–508.
- (47) Zoffmann, S.; Gether, U.; Schwartz, T. W. Conserved HisVI-17 of the NK-1 receptor is involved in binding of non-peptide antagonists but not substance P. *FEBS Lett.* **1993**, *336*, 506–510.
- (48) Huang, R. R.; Yu, H.; Strader, C. D.; Fong, T. M. Localization of the ligand binding site of the neurokinin-1 receptor: interpretation of chimeric mutations and single-residue substitutions. *Mol. Pharmacol.* **1994**, *45*, 690–695.
- (49) Huang, R. R.; Yu, H.; Strader, C. D.; Fong, T. M. Interaction of substance P with the second and seventh transmembrane domains of the neurokinin-1 receptor. *Biochemistry* **1994**, *33*, 3007–3013.

- (50) Greenfeder, S.; Cheewatrakoolpong, B.; Billah, M.; Egan, R. W.; Keene, E.; et al. The neurokinin-1 and neurokinin-2 receptor binding sites of MDL103,392 differ. *Bioorg. Med. Chem.* **1999**, *7*, 2867–2876.
- (51) Morris, G. M.; Goodsell, D. S.; Huey, R.; Olson, A. J. Distributed automated docking of flexible ligands to proteins: parallel applications of AutoDock 2.4. *J. Comput.-Aided Mol. Des.* **1996**, *10*, 293–304.
- (52) Natsugari, H.; Ikeura, Y.; Kiyota, Y.; Ishichi, Y.; Ishimaru, T.; et al. Novel, potent, and orally active substance P antagonists: synthesis and antagonist activity of *N*-benzylcarboxamide derivatives of pyrido[3,4-*b*]pyridine. *J. Med. Chem.* **1995**, *38*, 3106–3120.
- (53) Gerber, P. R.; Muller, K. MAB, a generally applicable molecular force field for structure modelling in medicinal chemistry. *J. Comput.-Aided Mol. Des.* **1995**, *9*, 251–268.
- (54) Gerber, P. R. Charge distribution from a simple molecular orbital type calculation and nonbonding interaction terms in the force field MAB. *J. Comput.-Aided Mol. Des.* **1998**, *12*, 37–51.
- (55) Oliveira, L.; Paiva, A. C.; Vriend, G. Correlated mutation analyses on very large sequence families. *ChemBioChem* **2002**, *3*, 1010–1017.
- (56) Weiner, S. J.; A., K. P.; Nguyen, D. T.; Case, D. An all atom force field for simulations of proteins and nucleic acids. *J. Comput. Chem.* **1986**, *7*, 230–252.
- (57) Hindle, S. A.; Rarey, M.; Buning, C.; Lengau, T. Flexible docking under pharmacophore type constraints. *J. Comput.-Aided Mol. Des.* **2002**, *16*, 129–149.
- (58) Brenk, R.; Naerum, L.; Gradler, U.; Gerber, H. D.; Garcia, G. A.; et al. Virtual screening for submicromolar leads of tRNA-guanine transglycosylase based on a new unexpected binding mode detected by crystal structure analysis. *J. Med. Chem.* **2003**, *46*, 1133–1143.
- (59) Gruneberg, S.; Stubbs, M. T.; Klebe, G. Successful virtual screening for novel inhibitors of human carbonic anhydrase: strategy and experimental confirmation. *J. Med. Chem.* **2002**, *45*, 3588–3602.
- (60) Oprea, T. I.; Davis, A. M.; Teague, S. J.; Leeson, P. D. Is there a difference between leads and drugs? A historical perspective. *J. Chem. Inf. Comput. Sci.* **2001**, *41*, 1308–1315.
- (61) Hann, M. M.; Leach, A. R.; Harper, G. Molecular complexity and its impact on the probability of finding leads for drug discovery. *J. Chem. Inf. Comput. Sci.* **2001**, *41*, 856–864.
- (62) Pan, Y.; Huang, N.; Cho, S.; MacKerell, A. D., Jr. Consideration of molecular weight during compound selection in virtual target-based database screening. *J. Chem. Inf. Comput. Sci.* **2003**, *43*, 267–272.
- (63) Stahl, M.; Rarey, M. Detailed analysis of scoring functions for virtual screening. *J. Med. Chem.* **2001**, *44*, 1035–1042.
- (64) Schulz-Gasch, T.; Stahl, M. Binding site characteristics in structure-based virtual screening: evaluation of current docking tools. *J. Mol. Model. (Online)* **2003**, *9*, 47–57.
- (65) Krämer, O.; Hazelmann, I.; Podjarny, A. D.; Klebe, G. Virtual screening for inhibitors of human aldose reductase. *Proteins* **2004**, *55*, 814–823.
- (66) Baker, D.; Sali, A. Protein structure prediction and structural genomics. *Science* **2001**, *294*, 93–96.
- (67) Ofner, S.; Hauser, K.; Schilling, W.; Vassout, A.; Veenstra, S. SAR of 2-benzyl-4-aminopiperidines: CGP-49823, an orally and centrally active non-peptide NK-1 antagonist. *Bioorg. Med. Chem.* **1996**, *6*, 1623–1628.
- (68) Williams, B. J.; Tcall, M.; McKenna, J. Acyclic NK-1 antagonists: 2-Benzhydryl-2-aminoethylethers. *Bioorg. Med. Chem. Lett.* **1994**, *4*, 1903–1908.
- (69) Desai, M. C.; Lefkowitz, S. L.; Thadeio, P. F.; Longo, K. P.; Snider, R. M. Discovery of a potent substance P antagonist: recognition of the key molecular determinant. *J. Med. Chem.* **1992**, *35*, 4911–4913.
- (70) Ladduwahetty, T.; Baker, R.; Cascieri, M. A.; Chambers, M. S.; Haworth, K.; et al. *N*-Heteroaryl-2-phenyl-3-(benzyloxy)piperidines: a novel class of potent orally active human NK1 antagonists. *J. Med. Chem.* **1996**, *39*, 2907–2914.
- (71) Stevenson, G. I.; MacLeod, A. M.; Huscroft, I.; Cascieri, M. A.; Sadowski, S.; et al. 4,4-Disubstituted piperidines: a new class of NK1 antagonist. *J. Med. Chem.* **1995**, *38*, 1264–1266.

JM0311487